

2020

Impact of DYRK1A Haploinsufficiency on Facial Morphology using Three-Dimensional Morphometric Analysis

Stefani Hammond

University of Central Florida, stefanihammond@knights.ucf.edu

 Part of the Anthropology Commons

Find similar works at: <https://stars.library.ucf.edu/urj>

University of Central Florida Libraries <http://library.ucf.edu>

This Article is brought to you for free and open access by the Office of Undergraduate Research at STARS. It has been accepted for inclusion in The Pegasus Review: UCF Undergraduate Research Journal (URJ) by an authorized editor of STARS. For more information, please contact STARS@ucf.edu.

Recommended Citation

Hammond, Stefani (2020) "Impact of DYRK1A Haploinsufficiency on Facial Morphology using Three-Dimensional Morphometric Analysis," *The Pegasus Review: UCF Undergraduate Research Journal (URJ)*: Vol. 12 : Iss. 1 , Article 3.

Available at: <https://stars.library.ucf.edu/urj/vol12/iss1/3>



Impact of *DYRK1A* Haploinsufficiency on Facial Morphology using Three-Dimensional Morphometric Analysis

By: Stefani Hammond

Faculty Mentor: Dr. Lana Willians

UCF Department of Anthropology

.....

ABSTRACT: Dual-specificity tyrosine-(Y)-phosphorylation regulated kinase 1A (DYRK1A) is a gene present on human chromosome 21. Previous research suggests that this gene plays a developmental role in facial morphology. We hypothesize that individuals with DYRK1A haploinsufficiency have altered facial morphology with potentially unique patterns of facial variation. To assess this hypothesis, we acquired three-dimensional (3D) photogrammetric facial images of individuals with and without DYRK1A haploinsufficiency, and we measured anatomical landmarks to carry out Euclidean Distance Matrix Analysis (EDMA) and to evaluate global and local morphological differences. Our results show unique patterns of variation between individuals with DYRK1A haploinsufficiency and normal siblings, as well as unrelated normal controls, supporting our hypothesis. These results identify exactly how and where DYRK1A haploinsufficiency changes patterns of facial morphology. Additionally, these results may have clinical relevance by identifying regions of the face that can benefit from early developmental interventions, therapeutic measures, or potentially plastic surgery.

KEYWORDS: DYRK1A; haploinsufficiency; biological anthropology; morphometrics

INTRODUCTION

Dual-specificity tyrosine-(Y)-phosphorylation regulated kinase 1A (*DYRK1A*) is a gene located on human chromosome 21 in the region 21q22.2 which produces the DYRK1A protein kinase (Fotaki et al., 2002; Singh & Lauth, 2017). The function of the DYRK1A protein is highly dependent on the dosage of the *DYRK1A* gene (Singh & Lauth, 2017). The DYRK1A protein has roles in many crucial cellular functions, including the regulation of cell life cycles, cell proliferation, differentiation, gene transcription and expression, and phosphorylation of other proteins (Soppa & Becker, 2015; Yoshida, 2008). Its expression in mammals is strongest during embryonic stages and decreases during postnatal periods, reaching its lowest levels during adulthood (Tejedor & Hämmerle, 2010; Yabut, Domogauer & D'Arcangelo, 2010). Expression in early postnatal stages is strongest in the central nervous system and the heart, while also affecting neural system development (Fernández-Martínez, Zahonero & Sánchez-Gómez, 2015). In the brain and nervous system, the protein is most expressed in areas controlling motor function (Dierssen & de Lagrán, 2006). In addition, DYRK1A has recently been proposed as the candidate gene for Autism Spectrum Disorder (ASD) and Intellectual Disability (ID) (Dang et al., 2017; van Bon et al., 2015).

While overexpression of *DYRK1A* in Trisomy 21 is characteristic of those with Down Syndrome, underexpression of *DYRK1A*, also known as *DYRK1A* haploinsufficiency, is caused by a partial or complete deletion of one copy of *DYRK1A*. Mammals without a functional copy of *DYRK1A* often die during prenatal development in the organogenesis period, possibly due to delayed organ growth and poor embryonic blood circulation (Fotaki et al., 2002). Most studies investigating this condition have used transgenic mice models with a focus on quantifiable changes in brain size, neural development, and impact on spatial reasoning (Arqué et al., 2008; Fotaki et al., 2002; Tejedor & Hämmerle, 2010). Studies involving human models for the condition are often case studies describing phenotypic variations of patients diagnosed with *DYRK1A* mutations. These phenotypic variations include deep set eyes, large or dysplastic ears, pointed nasal tip, long or flat philtrum, thin upper lip, and micrognathia (Bronicki et al., 2015; Ruaud et al., 2015; Ji et al., 2015). These variations, however, have not yet been quantified in human models.

The purpose of this study was to use three-dimensional (3D) images to assess whether the distinct facial morphology of those affected by *DYRK1A* haploinsufficiency is specific to the condition. We hypothesize that *DYRK1A* haploid individuals will exhibit fewer significant morphological differences when compared to euploid siblings than in comparisons to the unrelated euploid group. We also expect *DYRK1A* haploid individuals to exhibit more differences compared to both the euploid sibling and euploid control samples than are observed between the euploid sibling and euploid control. Through these comparisons, we expect to reveal patterns of dysmorphologies exclusive to the condition by identifying specific linear distances (LDs) that significantly differ in comparisons between *DYRK1A* haploid individuals, euploid siblings, and euploid controls.

METHODS AND MATERIALS

This study uses a small sample study design to analyze photogrammetric surface images of: 1) children with *DYRK1A* haploinsufficiency (hereafter referred to as the *DYRK1A* Haploid sample; $n = 20$), 2) unaffected euploid siblings of individuals with *DYRK1A* haploinsufficiency (hereafter referred to as the *DYRK1A*sib sample; $n = 11$), and 3) unaffected unrelated normal controls (hereafter referred to as the EU sample; $n = 120$) to assess facial morphology. Sex ratios between samples were similar but not identical (sample 1: 55% female, 45% male; sample 2: 36% female, 64% male; sample 3: 47.5% female, 52.5% male). Samples were also similar in age distribution (sample 1: range of 2-21 years of age, mean age of 10 ± 5.87 ; sample 2: range of 1-18 years of age, mean age of 11 ± 5.12 ; sample 3: range of 1-21 years of age, mean age 11 ± 4.70). The ethnicity for the majority of the individuals in each sample have either been self-identified or identified by a parent or guardian as Caucasian.

Photogrammetric images were previously acquired at local conferences and *DYRK1A* meetups for affected families using the 3dMD photogrammetric system 3dMD Patient. Multiple images of an individual's face were taken simultaneously and stitched together using 3dMD algorithms to create a single three-dimensional surface (Starbuck et al. 2017). This type of technology is ideal for phenotypic studies due to its ability to capture images noninvasively, quickly, and with replicable precision (Aldridge, Boyadjiev, Capone, DeLeon & Richtsmeier, 2005; Nord et al., 2015).

To assess measurement error of anatomical landmark placement, 21 anatomical soft tissue landmarks were collected repeatedly from ten individuals drawn randomly from the overall sample. Locations of landmarks and their corresponding labels and definitions are illustrated in Figure 1 and Table 1 of the Appendix. Using 3dMD Patient, each image was landmarked twice with at least 24 hours between sessions to avoid memory bias. The overall mean measurement error for this study was 0.065mm, which is considered sufficiently accurate for the purpose of this study.

After the analysis of measurement error provided satisfactory results, each of the sample images was landmarked in two separate trials at least 24 hours apart. Landmarks were inspected to evaluate for gross errors (e.g., swapping left and right side) and then averaged to further minimize measurement error. Seven images from the *DYRK1A* Haploid group and three images from the *DYRK1Asib* group provided by collaborators were too small to landmark in 3dMD software, so an alternative software (Amira) was used. Afterwards, each individual's anatomical landmark coordinates were scaled to the same centroid size using MorphoJ software. This process removed size variation so the LDs could be statistically assessed given the age variation and size differences of the collaborator images. Scaled anatomical landmark coordinates were then analyzed using Euclidean Distance Matrix Analysis (EDMA) and principal coordinates analysis (PCOORD) to assess local and global morphological differences.

Global patterns among samples were visualized using PCOORD, which summarizes and represents LD differences in a high-dimensional space to depict variation trends between samples, within samples, and between individuals (Bookstein, 1991; Starbuck et al., 2017). PCOORD uses form difference matrices (FDMs) of individuals as opposed to sample-wide FDMs. FDMs of two individuals are used to compute an F_{Ω} . An F_{Ω} is calculated for every unique pair of individuals, with an F_{Ω} of 0 suggesting that the two individuals have identical forms and F_{Ω} increasing as the two individuals become more different. The F_{Ω} for each pair is placed into a square matrix, which is then evaluated. The resulting values are used to place each individual on the axis of the resulting high-dimensional space. Ellipses formed by PCOORD analysis represent 70% confidence intervals.

EDMA is a morphometric technique that uses landmark data to calculate linear distances to estimate mean form

and mean form differences. Size and shape are quantified by calculating distances between all pairs of 21 landmarks, resulting in 210 unique LDs. A mean form matrix (FM) is computed to represent the mean distance between two landmarks across an entire sample. The FM is then used in a form difference matrix (FDM). The FDM uses ratios of mean forms of homologous LDs to quantify differences between samples by formatting them into the statistic $T = \max/\min$. The T statistic is used to test the null hypothesis of the LDs being identical. A T of one (or very close to one) would not provide sufficient evidence to reject the null hypothesis, while a T greater than 1 would provide sufficient evidence to reject the null hypothesis and suggest the LDs are significantly different (Lele, 1993; Starbuck et al., 2017). Local null hypotheses were evaluated using a nonparametric bootstrap (10,000 resamples) and confidence interval testing ($\alpha = 0.10$). Confidence intervals were then provided for each LD, where confidence intervals that did not contain 0 were reported as significantly different and confidence intervals that contained 0 were not reported as significant.

RESULTS

PCOORD Analysis

The PCOORD scatterplot is presented in Figure 3 of the Appendix. The results illustrate a slight overlap of all three samples in multivariate shape space. There is a large overlap present between the EU and *DYRK1Asib* groups, while there is less overlap between the *DYRK1A* Haploid group and the *DYRK1Asib* and EU groups. These overlaps imply that the *DYRK1Asib* and EU groups share similar ranges of facial morphology, while the *DYRK1A* Haploid group differs from both the *DYRK1Asib* or EU samples. In the *DYRK1A* Haploid group, the larger ellipse implies more variation within the sample. The larger ellipse size of the *DYRK1A* Haploid group compared to the ovals of the two other samples also implies greater variation in this sample compared to the other two groups.

EDMA Analysis

A summary of the EDMA analysis is presented in Table 2. The *DYRK1A* Haploid sample had fewer significant differences compared to the *DYRK1Asib* sample than to the EU sample. Approximately 36.7% (77/210) of LDs differed between the *DYRK1A* Haploid and *DYRK1Asib* samples, while 42.86% (90/210) of LDs differed between the *DYRK1A* Haploid and EU groups.

The greater similarity of the *DYRK1A* Haploid sample to the *DYRK1A*sib sample is expected due to the implied genetic similarities between these groups. 8.1% (17/210) of LDs were significantly different between *DYRK1A*sibs and EU, which are both genetically normal.

LDs that were found to be different are visualized in Figure 2 of the Appendix. LDs present in the comparisons of *DYRK1A* Haploid to *DYRK1A*sib are largely similar to LDs present when comparing the *DYRK1A* Haploid and the EU group. When directly comparing the different LDs between the two sets of comparisons, there are 28 LDs exclusive to the *DYRK1A* Haploid v. *DYRK1A*sib and *DYRK1A* Haploid v. EU groups. These distances can be attributed to the effect of *DYRK1A* haploinsufficiency, suggesting substantial differences in facial form due to *DYRK1A* haploinsufficiency. Most of these LDs are in the midfacial region, focused around the nose and philtrum.

DISCUSSION

Development of the craniofacial complex involves several different factors and their interactions, including underlying genes and prenatal environment (Johnston & Bronsky, 1995; Starbuck et al. 2017). Mechanisms affected by these factors, which can result in craniofacial dysmorphologies, include brain patterning, cell migration, tissue fusion and bone differentiation. Cell proliferation and cell migration are the most common mechanisms of the development of craniofacial morphology (Wilkie & Morriss-Kay, 2001). Because a large part of the *DYRK1A* protein's role involves cell proliferation, proper dosage of the *DYRK1A* gene is crucial for proper craniofacial development.

As a signaling molecule, the *DYRK1A* protein also affects the development of the neural crest, which later develops into embryonic facial organs (Francis-West, Ladher, Barlow & Graveson, 1998; Szabo-Rogers, Smithers, Yakob & Liu, 2010). Craniofacial development begins with the cranial fossae (where the brain rests within the skull), followed by reduction of the interorbital distance (distance between the eyes), and growth of the nasomaxillary complex (upper jaw and nasal cavity) (van der Meulen, Mazzola, Vermey-Keers, Strieker & Raphael, 1983). Many of these regions are also found to likely be affected by *DYRK1A* haploinsufficiency, especially those in the nasomaxillary complex. This finding implies that changes in dosage of *DYRK1A* affect craniofacial development beginning in its early stages.

Both the EDMA and PCOORD results support the conclusion that *DYRK1A* Haploinsufficiency affects facial morphology in a manner that obscures even familial similarities. The ellipse of the *DYRK1A* Haploid group in the PCOORD analysis is larger than the ellipses of the two other samples, implying more variation within the sample compared to the other two groups. The greater variation in the *DYRK1A* Haploid group is likely due to this genetic deficiency and its effect on development. The degree of morphological difference between the *DYRK1A* Haploid and *DYRK1A*sib group implies that despite these groups' shared DNA, the condition affects craniofacial morphology to the extent what it obscures facial resemblance. While these changes do seem to obscure most familial resemblance, the fewer significant differences between the *DYRK1A*sibs sample compared to the EU sample imply that not all shared genetic resemblance is lost due to the condition.

This study's identification of patterns of dysmorphology in those affected by *DYRK1A* haploinsufficiency support findings from case studies describing common traits found in patients with the condition, including thin upper lip, long philtrum, and pointed nasal tip, as these are found in the nasomaxillary complex. Defects affecting the central facial region could potentially impact quality of life, as organs in this region are the main mode of facial expression. Moreover, reconstruction in these areas often poses difficulties due to their complexity and the extent to which features are connected (Ratner & Levender, 2013).

While this study focuses on soft-tissue morphology of human models, the lack of quantifiable data in human models means it is difficult to support many conclusions presented in the current literature on this condition. While some comparisons can be drawn to quantifiable studies using mouse models, these studies lack information on soft tissue morphology. To develop a greater understanding of the extent that *DYRK1A* haploinsufficiency affects facial morphology, further research in human models should be conducted with a focus on quantitative studies on soft tissue and bone. Further research in mouse models with focuses on quantitative studies of skull morphology might also prove beneficial. Due to limitations in this study of relatively limited sample size and ethnic diversity, it would be advantageous for future studies to both increase sample size and seek out greater diversity in the sample groups.

CONCLUSION

Our results, based on the sheer number of facial differences, support our hypothesis that *DYRK1A* plays an important role in facial development. Here we have shown that *DYRK1A* expression alters soft-tissue morphology, but it is unknown if these changes occurred due to underlying bone changes or in combination with them. Middle and lower face morphology may be impacted by impaired growth and fusion of the maxillary, nasal, and mandibular prominences during development. Since skin is biologically built upon the bony scaffold of the skull, connective tissues may be altered by *DYRK1A* underexpression as well. Many individuals with *DYRK1A* haploinsufficiency also suffer from cognitive impairment, implying that brain development may also be impacted. Future studies should assess bone and brain morphology using human or animal model samples to differentiate and elucidate the primary and secondary effects of *DYRK1A* haploinsufficiency upon these tissues.

APPENDIX

Figure 1. An example of landmarks placed on individual in 3dMD patient

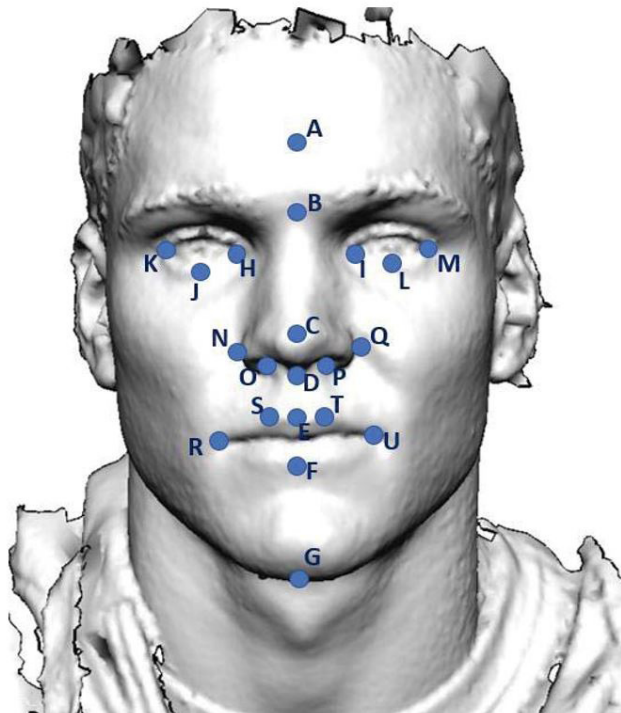


Table 1. Landmark labels and their anatomical definitions

LABEL	ANATOMICAL LANDMARK DEFINITION
A	Glabella: Midpoint between the eyebrows on the median plane
B	Sellion: Deepest point of the nasal root
C	Pronasale: Most anterior point of the nose tip
D	Subnasale: Point where the nasal septum meets the philtrum
E	Labiale superius: Midpoint of the vermillion seam of the upper lip
F	Labiale inferius: Midpoint of the vermillion seam of the lower lip
G	Gnathion: Most inferior point of the chin
H	Endocanthion R: Point located in the inner commissure of the eye (right)
I	Endocanthion L: Point located in the inner commissure of the eye (left)
J	Palpebrae inferius R: Most inferior point of the lower eyelid (right)
K	Exocanthion R: Point located in the outer commissure of the eye (right)
L	Palpebrae inferius L: Most inferior point of the lower eyelid (left)
M	Exocanthion L: Point located in the outer commissure of the eye (left)
N	Alare R: Most lateral point of the nasal wings (right)
O	Subalare R: The facial insertion of the alar base (right)
P	Subalare L: The facial insertion of the alar base (left)
Q	Alare L: Most lateral point of the nasal wings (left)
R	Chelion R: Point located in the labial commissure (right)
S	Crista philtra R: Crossing of the vermillion line and elevated margin of the philtrum (right)
T	Crista philtra L: Crossing of the vermillion line and elevated margin of the philtrum (left)
U	Chelion L: Point located in the labial commissure (left)

Table 2. Summary of EDMA shape analysis results. A total of 210 linear distances were statistically evaluated for each pairwise sample comparison.

Samples Compared	Percentage of Significant Measurements
<i>DYRK1A</i> Haploid compared to EU	42.86% (90/210)
<i>DYRK1A</i> Haploid compared to <i>DYRK1A</i> sibs	36.7% (77/210)
EU compared to <i>DYRK1A</i> sibs	8.1% (17/210)

Figure 2. A) Significant differences between the *DYKR1A* haploid and EU samples, B) Significant differences between the *DYKK1A* Haploid and *DYRK1A*sib samples, and C) Significant differences between the EU and *DYRK1A*sib samples. Facial images shown have been modified to remove identifiable features.

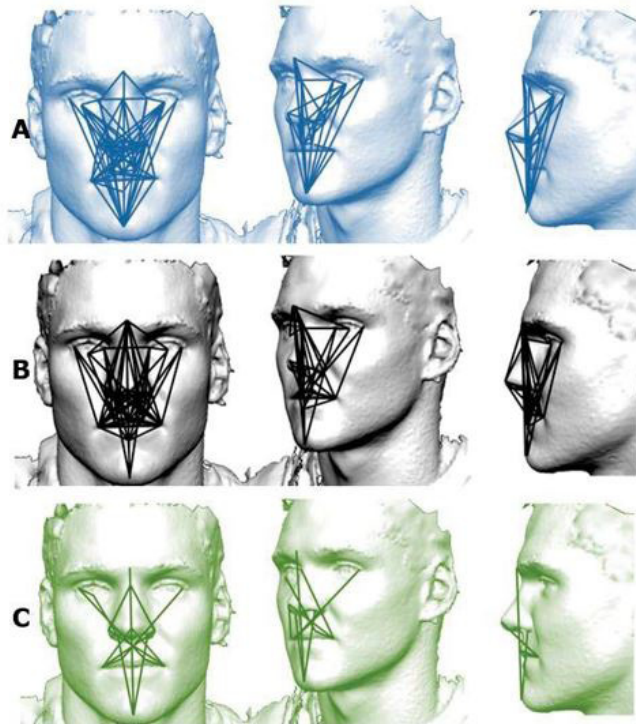
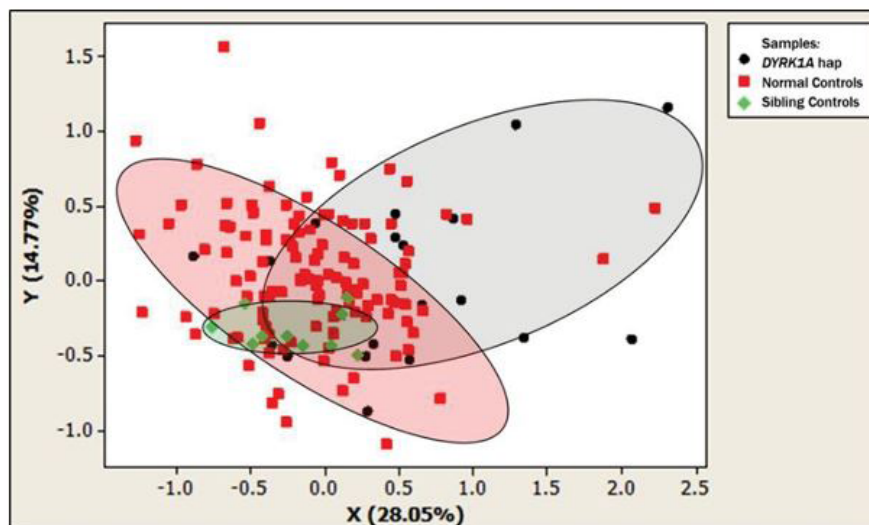


Figure 3. Results from an EDMA PCOORD analysis. The farther apart two individuals along one axis, the greater the difference in form. In summary, 28.05% of the variance is explained by the X axis, whereas the Y axis explains 14.77% of the variance across the samples.



REFERENCES

- Aldridge, K., Boyadjiev, S., Capone, G., DeLeon, V., & Richtsmeier, J. (2005). *Precision and error of three-dimensional phenotypic measures acquired from 3dMD photogrammetric images*. *American Journal Of Medical Genetics Part A*, 138A(3), 247-253. doi: 10.1002/ajmg.a.30959
- Arqué, G., Fotaki, V., Fernández, D., de Lagrán, M., Arbonés, M., & Dierssen, M. (2008). *Impaired Spatial Learning Strategies and Novel Object Recognition in Mice Haploinsufficient for the Dual Specificity Tyrosine-Regulated Kinase-1A (Dyrk1A)*. *Plos ONE*, 3(7), e2575. doi: 10.1371/journal.pone.0002575
- Bookstein F. L. (1991). *Morphometric tools for landmark data geometry and biology*. Australia: Cambridge University Press.
- Bronicki, L., Redin, C., Drunat, S., Piton, A., Lyons, M., & Passemard, S. et al. (2015). *MG- 112 Ten new cases further delineate the syndromic intellectual disability phenotype caused by mutations in DYRK1A*. *Journal Of Medical Genetics*, 52(Suppl 1), A2.3-A3. doi: 10.1136/jmedgenet-2015-103577.6
- Dang, T., Duan, W., Yu, B., Tong, D., Cheng, C., & Zhang, Y. et al. (2017). *Autism-associated Dyrk1a truncation mutants impair neuronal dendritic and spine growth and interfere with postnatal cortical development*. *Molecular Psychiatry*, 23(3), 747-758. doi: 10.1038/mp.2016.253
- Dierssen, M., & de Lagrán, M. (2006). *1DYRK1A (Dual-Specificity Tyrosine-Phosphorylated and -Regulated Kinase 1A): A Gene with Dosage Effect During Development and Neurogenesis*. *TSW Development & Embryology*, 1, 87-98. doi: 10.1100/tswde.2006.120
- Fernández-Martínez, P., Zahonero, C., & Sánchez-Gómez, P. (2015). *DYRK1A: the double-edged kinase as a protagonist in cell growth and tumorigenesis*. *Molecular & Cellular Oncology*, 2(1), e970048. doi: 10.4161/23723548.2014.970048
- Fotaki, V., Dierssen, M., Alcantara, S., Martinez, S., Marti, E., & Casas, C. et al. (2002). *Dyrk1A Haploinsufficiency Affects Viability and Causes Developmental Delay and Abnormal Brain Morphology in Mice*. *Molecular And Cellular Biology*, 22(18), 6636-6647. doi: 10.1128/mcb.22.18.6636-6647.2002
- Francis-West, P., Ladher, R., Barlow, A., & Graveson, A. (1998). *Signalling interactions during facial development*. *Mechanisms Of Development*, 75(1-2), 3-28. doi: 10.1016/s0925-4773(98)00082-3
- Hämmerle, B., Elizalde, C., & Tejedor, F. (2008). *The spatio-temporal and subcellular expression of the candidate Down syndrome gene Mnb/Dyrk1A in the developing mouse brain suggests distinct sequential roles in neuronal development*. *European Journal Of Neuroscience*, 27(5), 1061-1074. doi: 10.1111/j.1460-9568.2008.06092.x
- Ji, J., Lee, H., Argiropoulos, B., Dorrani, N., Mann, J., & Martinez-Agosto, J. et al. (2015). *DYRK1A haploinsufficiency causes a new recognizable syndrome with microcephaly, intellectual disability, speech impairment, and distinct facies*. *European Journal Of Human Genetics*, 23(11), 1473-1481. doi: 10.1038/ejhg.2015.71
- Johnston, M., & Bronsky, P. (1995). *Prenatal Craniofacial Development: New Insights on Normal and Abnormal Mechanisms*. *Critical Reviews In Oral Biology & Medicine*, 6(4), 368-422. doi: 10.1177/10454411950060040601
- Nord, F., Ferjencik, R., Seifert, B., Lanzer, M., Gander, T., & Matthews, F. et al. (2015). *The 3dMD photogrammetric photo system in cranio-maxillofacial surgery: Validation of interexaminer variations and perceptions*. *Journal Of Cranio-Maxillofacial Surgery*, 43(9), 1798-1803. doi: 10.1016/j.jcms.2015.08.017
- Ratner, D., & Levender, M. (2013). *Reconstructing Complex Central Facial Defects Involving Multiple Cosmetic Subunits*. *Facial Plastic Surgery*, 29(05), 394-401. doi: 10.1055/s-0033-1353380
- Ruaud, L., Mignot, C., Guët, A., Ohl, C., Nava, C., & Héron, D. et al. (2015). *DYRK1A mutations in two unrelated patients*. *European Journal Of Medical Genetics*, 58(3), 168-174. doi: 10.1016/j.ejmg.2014.12.014
- Singh, R., & Lauth, M. (2017). *Emerging Roles of DYRK Kinases in Embryogenesis and Hedgehog Pathway Control*. *Journal Of Developmental Biology*, 5(4), 13. doi: 10.3390/jdb5040013
- Soppa, U., & Becker, W. (2015). *DYRK protein kinases*. *Current Biology*, 25(12), R488- R489. doi: 10.1016/j.

cub.2015.02.067

18. Starbuck, J., Cole, T., Reeves, R., & Richtsmeier, J. (2017). *The Influence of trisomy 21 on facial form and variability*. American Journal Of Medical Genetics Part A, 173(11), 2861-2872. doi: 10.1002/ajmg.a.38464

19. Szabo-Rogers, H., Smithers, L., Yakob, W., & Liu, K. (2010). *New directions in craniofacial morphogenesis*. Developmental Biology, 341(1), 84-94. doi: 10.1016/j.ydbio.2009.11.021

20. Tejedor, F., & Hämmerle, B. (2010). *MNB/DYRK1A as a multiple regulator of neuronal development*. FEBS Journal, 278(2), 223-235. doi: 10.1111/j.1742-4658.2010.07954.x

21. van Bon, B., Coe, B., Bernier, R., Green, C., Gerdtts, J., & Witherspoon, K. et al. (2015). *Disruptive de novo mutations of DYRK1A lead to a syndromic form of autism and ID*. Molecular Psychiatry, 21(1), 126-132. doi: 10.1038/mp.2015.5

22. van der Meulen, J., Mazzola, R., Vermey-Keers, C., Strieker, M., & Raphael, B. (1983). *A Morphogenetic Classification of Craniofacial Malformations*. Plastic And Reconstructive Surgery, 71(4), 560-572. doi: 10.1097/00006534-198304000-00022

23. Wilkie, A., & Morriss-Kay, G. (2001). *Genetics of craniofacial development and malformation*. Nature Reviews Genetics, 2(6), 458-468. doi: 10.1038/35076601

24. Yabut, O., Domogauer, J., & D'Arcangelo, G. (2010). *Dyrk1A Overexpression Inhibits Proliferation and Induces Premature Neuronal Differentiation of Neural Progenitor Cells*. Journal Of Neuroscience, 30(11), 4004-4014. doi: 10.1523/jneurosci.4711-09.2010

25. Yoshida, K. (2008). *Role for DYRK family kinases on regulation of apoptosis*. Biochemical Pharmacology, 76(11), 1389-1394. doi: 10.1016/j.bcp.2008.05.021